

# Structural and electrical properties of $\text{Nd}_{1.7}\text{Ba}_{0.3}\text{Ni}_{0.9}\text{Cr}_{0.1}\text{O}_{4+\delta}$ compound

Manel Jammali,<sup>1</sup> Rached Ben Hassen,<sup>1,a)</sup> and Jan Rohlicek<sup>2</sup>

<sup>1</sup>Unité de Recherche de Chimie des Matériaux et de l'Environnement(UR11ES25), ISSBAT, Université de Tunis El Manar, 9, Avenue Dr. Zoheir Safi, 1006 Tunis, Tunisie

<sup>2</sup>Institute of Physics ASCR, v.v.i, Na Slovance 2, 18221 Prague 8, Czech Republic

(Received 10 February 2012; accepted 17 April 2012)

The  $\text{Nd}_{1.7}\text{Ba}_{0.3}\text{Ni}_{0.9}\text{Cr}_{0.1}\text{O}_{4+\delta}$  polycrystalline sample was synthesized by the sol–gel process and a subsequent annealing at 1523 K in 1 atm of flowing argon. X-ray diffraction (XRD) analysis and electrical transport properties have been investigated as well. The oxygen non-stoichiometry was determined by iodometric titration. The sample shows adoption of the  $\text{K}_2\text{NiF}_4$ -type structure based on a tolerance factor calculation. Rietveld refinement of the crystal structure from X-ray powder diffraction data confirmed that  $\text{Nd}_{1.7}\text{Ba}_{0.3}\text{Ni}_{0.9}\text{Cr}_{0.1}\text{O}_{4+\delta}$  adopts the tetragonal structure (space group  $I4/mmm$ ,  $Z = 2$ ). The room temperature unit-cell parameters are determined to be  $a = 3.82515(2)$  and  $c = 12.47528(6)$  Å. The reliability factors are:  $R_B = 0.043$ ,  $R_{wp} = 0.012$  and  $\chi^2 = 3.00$ . The  $\text{Nd}_{1.7}\text{Ba}_{0.3}\text{Ni}_{0.9}\text{Cr}_{0.1}\text{O}_{4+\delta}$  compound exhibits a semi-conductive behaviour. The electrical transport mechanism has been investigated and it agrees with the adiabatic small polaron hopping model in the temperature range  $313 \text{ K} \leq T \leq 708 \text{ K}$ . © 2012 International Centre for Diffraction Data. [doi:10.1017/S0885715612000474]

Key words: X-ray diffraction,  $\text{K}_2\text{NiF}_4$ -type structure, sol–gel, Rietveld refinement, adiabatic small polaron hopping model, semi-conductive behaviour, iodometric titration

## I. INTRODUCTION

Many mixed oxides of the type  $\text{A}_2\text{BO}_4$  ( $A$  = rare earth, alkaline earth;  $B$  = transition metal) crystallize with the  $\text{K}_2\text{NiF}_4$ -type structure that can be described as an ordered intergrowth alternating perovskite ( $\text{ABO}_3$ ) and rock salt ( $\text{AO}$ ) layers. The  $\text{BO}_6$  octahedra share corners, forming a two-dimensional array of  $B\text{--O--B}$  bonds which is responsible for a variety of interesting physical phenomena, such as, the anisotropic electrical transport and magnetic exchange interactions (Bassat *et al.*, 1987; Buttrey and Honig, 1988). Rare earth nickelates show a considerable range of oxygen non-stoichiometry depending on their synthetic preparations (Arbuckle *et al.*, 1990). The excess of oxygen is attributed to intergrowth of Ruddelsden–Popper-type phases (Odier *et al.*, 1985), variable valence of the transition metal ion and more recently to the incorporation of interstitial oxygen defects (Jorgensen *et al.*, 1989). The structural and magnetic properties of  $\text{Ln}_2\text{NiO}_{4+\delta}$ -type compounds were reported to be extremely sensitive to the deviations in the oxygen stoichiometry (Buttrey *et al.*, 1986; Buttrey and Honig, 1988; Rodriguez-Carvajal *et al.*, 1988; Demourgues *et al.*, 1993).

It was reported that  $\text{Nd}_2\text{NiO}_{4+\delta}$  can have either monoclinic or orthorhombic symmetry. The source of the structural difference is unclear; it may be because of the oxygen content or structural defects (Arbuckle *et al.*, 1990). It was also reported that  $\text{NdSrNiO}_4$  has tetragonal symmetry (Takeda *et al.*, 1992). It was thought that the substitution of Nd by Sr in  $\text{Nd}_2\text{NiO}_{4+\delta}$  might induce a structural phase transition from orthorhombic to tetragonal symmetry leading to a mixed valence for the transition metal ion, which would in turn induce interesting electrical and magnetic properties in this system.

The layered  $\text{K}_2\text{NiF}_4$ -type  $\text{Ln}_{2-x}\text{Sr}_x\text{NiO}_{4-\delta}$  solid solutions for  $\text{Ln} = \text{La}, \text{Nd}, \text{Pr}, \text{Sm}$  and  $\text{Gd}$  have been extensively studied (Gopalakrishnan *et al.*, 1977; Arbuckle *et al.*, 1990; Sreedhar and Rao, 1990; Takeda *et al.*, 1990, 1992; Chen *et al.*, 1993). A unique set of these properties makes them useful as electrode materials in different electrochemical devices. Further investigations into these oxides have been carried out to find appropriate compositions with the best set of necessary properties.

Takeda *et al.* (1992) investigated the structural and physical properties of the  $\text{Nd}_{2-x}\text{A}_x\text{NiO}_4$  systems ( $A = \text{Ca}, \text{Sr}, \text{or Ba}$ ). The solid solution limits of alkaline earth were 0.6, 1.4 and 0.6 for Ca, Sr and Ba, respectively. In spite of the substitution of different alkaline earth metals, the distances of Ni–O showed no dependence with this action. The effect of this substitution was reflected on the Nd/Ca–O and Nd/Ba–O distances along the  $c$ -axis. The neodymium alkaline earth nickelates, therefore give good insights into the evolution of the perovskite structure owing to the deformation of the  $A$  site, resulting from the above-mentioned substitution. All  $\text{Nd}_{2-x}\text{Ca}_x\text{NiO}_4$  samples have the orthorhombic ( $Bmab$  and  $Fmmm$ ) structure. For  $\text{Nd}_{2-x}\text{Sr}_x\text{NiO}_4$  and  $\text{Nd}_{2-x}\text{Ba}_x\text{NiO}_4$ , there were tetragonal  $I4/mmm$  phases. A semiconductor–metal transition was observed for  $0 < x < 1.0$  in  $\text{Nd}_{2-x}\text{Sr}_x\text{NiO}_4$  systems, the transition temperature decreased from 450 K ( $x = 0.1$ ) to 100 K ( $x = 1.0$ ), but it exhibited a change in characteristic at  $x = 0.6$ .

In our previous works we successfully prepared neodymium  $\text{NdSrNi}_{1-x}\text{Cu}_x\text{O}_{4-\delta}$   $0 \leq x \leq 1$  and studied their structural and electrical properties (Chaker *et al.*, 2004, 2006). After that an investigation into the quaternary  $\text{Ln}_2\text{O}_3\text{--SrO--NiO--CuO}$  system showed a similar structure for  $\text{LnSr}_5\text{Ni}_{2.4}\text{Cu}_{0.6}\text{O}_{12-\delta}$  with the smaller lanthanides cations Dy, Ho and Er (Chaker *et al.*, 2007; Hamdi *et al.*, 2011).

Tonus *et al.* (2010) recently introduced a combination of nickel and chromium into the  $\text{K}_2\text{NiF}_4$  structure by synthesizing  $\text{Ln}_{3-x}\text{Sr}_{1+x}\text{NiCrO}_{8-\delta}$  ( $\text{Ln} = \text{La}, \text{Nd}$ ) with the aim of

<sup>a)</sup>Author to whom correspondence should be addressed. Electronic mail: rached.benhassen@fss.rnu.tn

identifying potential anode materials for Solid Oxide Fuel Cells (SOFCs). Their approach of selecting Cr/Ni-based compositions was influenced by the relative success of the analogous perovskite system. This stems firstly from the stability of  $\text{Cr}^{3+}$  to hydrogen reduction and the structural stability that this confers. Secondly, it relies on the electrocatalytic properties of the Ni cation and its ability to lower its oxidation state and coordination number to generate the oxygen-vacancy network needed for anionic conduction.

As, we are much more interested in mixed oxides based on neodymium, we have recently studied the series  $\text{NdSrNi}_{1-x}\text{Cr}_x\text{O}_{4+\delta}$ ,  $0 \leq x \leq 1$  (Jammali *et al.*, 2010) and the transport mechanism in this series was investigated. Our results found that these compounds exhibit a poor semi-conductive behaviour.

The aim of this work is to investigate the effect of chromium incorporation on the structural and physical properties of  $\text{Nd}_{2-x}\text{Ba}_x\text{NiO}_{4+\delta}$  systems with a bigger amount of alkaline earth which have not yet been reported. In this work, we report the results of powder X-ray diffraction (XRD) analysis, oxygen-content determination and electrical measurements of  $\text{Nd}_{1.7}\text{Ba}_{0.3}\text{Ni}_{0.9}\text{Cr}_{0.1}\text{O}_{4+\delta}$ .

## II. EXPERIMENTAL

### A. Synthesis

The  $\text{Nd}_{1.7}\text{Ba}_{0.3}\text{Ni}_{0.9}\text{Cr}_{0.1}\text{O}_{4+\delta}$  sample was prepared in polycrystalline form by sol-gel route. Stoichiometric quantities of  $\text{Nd}_2\text{O}_3$  (Aldrich 99.99%), pre-dried in air at 1223 K to remove any hydrogeno-carbonate impurities,  $\text{BaCl}_2 \cdot 2\text{H}_2\text{O}$  (Aldrich 99.99%),  $\text{Cr}(\text{NO}_3)_3 \cdot 9\text{H}_2\text{O}$  (Aldrich 99.99%) and NiO (Aldrich 99.99%), as appropriate, were dissolved in a minimum quantity, typically 150 ml, of a 1:1 solution of analAR 6-M nitric acid and distilled water. For each mole of transition metal, 3-mol equivalents of citric acid ( $\text{C}_6\text{H}_8\text{O}_7$ , 98%) solution were added along with 5 ml of ethylene glycol. The stirred solution was heated on a hot plate and the liquid evaporated gradually. A gel was formed and then dehydrated on a hot plate until a black powder residue remained. This residue was ground and calcined in a furnace at 1073 K for 12 h to remove the remaining organic component. The resultant powder was subsequently ground and heated in argon at 1523 K for 96 h. In between the sintering steps, the sample was cooled and then grounded.

### B. Data collection and electrical measurements

Powder XRD pattern of the new compound was collected at room temperature using a Diffractometer Empyrean of PANalytical equipped with an incident-beam curved Ge (111) Johansson monochromator to obtain  $\text{Cu K}\alpha_1$  radiation ( $\lambda = 1.54056 \text{ \AA}$ ). Data were collected at each  $0.007^\circ$  step width, for 50 s over a  $2\theta$  range from  $10.003$  to  $150.017^\circ$ , and a PIXcel<sup>3D</sup> solid-state X-ray detector was used in the Bragg-Brentano geometry.

Direct current resistivity measurements were carried out on sintered pellets using a Lucas Labs 302 four-point probe with a Keithley 2400 digital Source Meter (Keithley Instruments Inc., Cleveland, Ohio). Measurements were performed in the temperature range between 313 and 708 K.

The oxygen content of the single-phase powder was indirectly determined at room temperature after calculation of the valence average of the transition metal ions obtained by iodometric titration. In fact, about 50 mg of the sample were dissolved in a solution of 6-M hydrochloric acid in the presence of excess KI, leading to reduction of tri- and tetrametal transition ions and formation of iodine that was titrated with  $\text{Na}_2\text{S}_2\text{O}_3$  solution using starch as indicator. The sodium thiosulfate solution was standardized using pure copper wire.

## III. RESULTS AND DISCUSSION

### A. Crystal structure and oxygen content

The purity of the prepared sample was confirmed by laboratory powder XRD measurements, which revealed neither impurities nor starting materials.

The most intense observed lines in the pattern of the new phase were selected to establish the procedure of indexing by means of DICVOL91 program (Boultif and Lauër, 1991). It was found that  $\text{Nd}_{1.7}\text{Ba}_{0.3}\text{Ni}_{0.9}\text{Cr}_{0.1}\text{O}_{4+\delta}$  adopts the tetragonal  $\text{K}_2\text{NiF}_4$ -type structure with  $I4/mmm$  space group. The refined unit-cell parameters are listed in Table I.

The Rietveld refinement was carried out with the pseudo-Voigt function used for the simulation of peak shapes. First, we started with refinement of the zero-point instrument, unit-cell parameters, half-width parameters  $U$ ,  $V$ ,  $W$  and then, the background was fitted with a linear interpolation between 99 chosen points. The structural refinement was carried out in the space group  $I4/mmm$  with Nd/Ba and O(2) atoms [situated at special positions 4e with coordinates (0, 0, z)]. The Ni and Cr atoms are located at (0, 0, 0) in the 2a site and the O(1) atoms at (0,  $\frac{1}{2}$ , 0) in the 4c site. Atomic positions have been refined for all the atoms, together with the scale factor and profile parameters. The refinements of all isotropic temperature factors including those of oxygen were stable, and the least square analysis converged quickly to provide a good fit to the diffraction pattern.

It was impossible to refine the Ni/Cr ratio, owing to the similar X-ray scattering powers of these elements. The refinements of the isotropic temperature factors were unstable, but good results were obtained by refinement of overall isotropic displacement factor. Finally, refinement of the preferred orientation correction in the [001]-direction led to a highly significant diminution of  $\chi^2$ , and a considerable improvement in the quality of the fit. A final refinement converged to  $R_B = 4.37\%$ ,  $R_{wp} = 12.2\%$  and  $\chi^2 = 3.00$ ,  $R_p = 15.2\%$  and  $R_F = 4.38\%$ . The Rietveld refinement procedures were used with the help of the FULLPROF software (Rodríguez-Carvajal, 1990).

The stability of the  $\text{Nd}_{1.7}\text{Ba}_{0.3}\text{Ni}_{0.9}\text{Cr}_{0.1}\text{O}_{4+\delta}$  compound having the  $\text{K}_2\text{NiF}_4$ -type structure can be discussed in terms

TABLE I. Crystal data for  $\text{Nd}_{1.7}\text{Ba}_{0.3}\text{Cr}_{0.1}\text{Ni}_{0.9}\text{O}_{4+\delta}$ .

Chemical composition	$\text{Nd}_{1.7}\text{Ba}_{0.3}\text{Cr}_{0.1}\text{Ni}_{0.9}\text{O}_{4+\delta}$
Space group	$I4/mmm$
$a$ ( $\text{\AA}$ )	3.82515(2)
$c$ ( $\text{\AA}$ )	12.47528(6)
$V$ ( $\text{\AA}^3$ )	182.535(1)
$Z$	2
$D_x$ ( $\text{g cm}^{-3}$ )	7.43

of the value of the tolerance factor defined by Goldschmidt (Ganguly and Rao, 1984) as

$$t = \frac{(1.7r_{\text{Nd}^{3+}} + 0.3r_{\text{Ba}^{2+}})}{2} + r_0^{2-} / \sqrt{2[0.9r_{\text{Ni}^{3+}} + 0.1r_{\text{Cr}^{3+}} + r_0^{2-}]}$$

The  $\text{K}_2\text{NiF}_4$ -type structure is stable over the range  $0.866 \leq t < 1$ . The T (tetragonal) structure exists for  $0.88 \leq t \leq 0.99$  and the T/O (tetragonal/orthorhombic) structure is present for  $0.866 \leq t < 0.88$ . Based on Shannon's ionic radii (Shannon, 1976) ( $r_{\text{Nd}^{3+}} = 1.163 \text{ \AA}$ ,  $r_{\text{Ba}^{2+}} = 1.47 \text{ \AA}$  in a 9-fold coordination and  $r_{\text{Ni}^{3+}} = 0.56 \text{ \AA}$ , in the low-spin case,  $r_{\text{Cr}^{3+}} = 0.615 \text{ \AA}$  and  $r_{\text{O}^{2-}} = 1.4 \text{ \AA}$  in a 6-fold coordination), the theoretical tolerance factor for  $\text{Nd}_{1.7}\text{Ba}_{0.3}\text{Ni}_{0.9}\text{Cr}_{0.1}\text{O}_{4+\delta}$  is  $t = 0.938$ , this value was included in the tetragonal symmetry stability range. Consequently, refinement of  $\text{Nd}_{1.7}\text{Ba}_{0.3}\text{Ni}_{0.9}\text{Cr}_{0.1}\text{O}_{4+\delta}$  X-ray data has been performed to confirm the  $\text{K}_2\text{NiF}_4$ -type structure.

To study the variation in the oxygen content, we carried out iodometric titration using  $\text{Na}_2\text{S}_2\text{O}_3$  standard solution. The oxygen non-stoichiometry ( $\delta$ ) is directly correlated to the  $\text{Ni}^{3+}$  and  $\text{Cr}^{4+}$  content according to the formulation  $\text{Nd}_{1.7}\text{Ba}_{0.3}(\text{Ni}_{1-\tau}^{3+} \text{Ni}_{\tau}^{2+})_{0.9}(\text{Cr}_{1-\tau}^{4+} \text{Cr}_{\tau}^{3+})_{0.1}\text{O}_{4+\delta}$ , with  $\delta = (0.8 - \tau)/2$ . The content  $(1 - \tau)$  of the average of cation transition metals  $\text{Ni}^{3+}$  and  $\text{Cr}^{4+}$  was determined by iodometric titration.  $\text{I}^-$  anions reduce  $\text{dNi}^{3+}$  cations into  $\text{Ni}^{2+}$  and reduce  $\text{Cr}^{4+}$  cations into  $\text{Cr}^{3+}$ . The titration of the resulting  $\text{I}_2$ , by a solution of  $\text{Na}_2\text{S}_2\text{O}_3$  sodium thiosulfate led, by considering the average of cations transition metals  $\text{Ni}^{3+}$  and  $\text{Cr}^{4+}$ , to the value  $\tau = 0.67$  and therefore  $\delta = 0.06$ , indicating excess oxygen in the sample.

## B. Structure description

The observed, calculated and difference profiles for the Rietveld refinement of  $\text{Nd}_{1.7}\text{Ba}_{0.3}\text{Ni}_{0.9}\text{Cr}_{0.1}\text{O}_{4+\delta}$  compound are shown in Figure 1. The structurally refined parameters for  $\text{Nd}_{1.7}\text{Ba}_{0.3}\text{Ni}_{0.9}\text{Cr}_{0.1}\text{O}_{4+\delta}$  are summarized in Table II.

As shown in Figure 2, the structure of  $\text{Nd}_{1.7}\text{Ba}_{0.3}\text{Ni}_{0.9}\text{Cr}_{0.1}\text{O}_{4+\delta}$  sample can be described as an ordered intergrowth of alternating perovskite  $(\text{Nd/Ba})(\text{Ni/Cr})\text{O}_3$  and rock salt  $(\text{Nd/Ba})\text{O}$  layers stacked along the tetragonal  $c$ -axis.

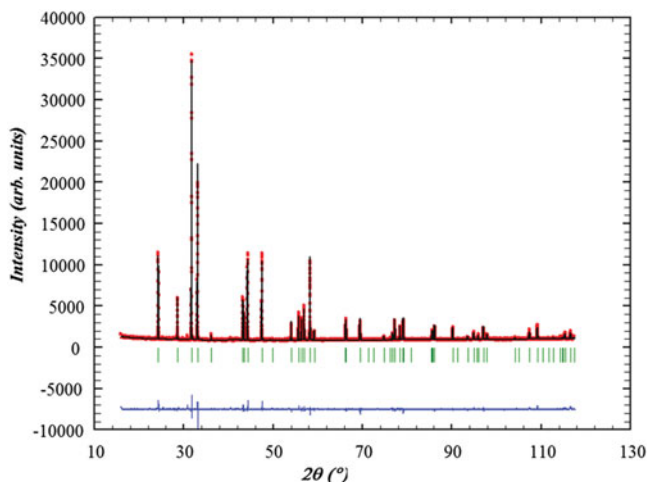


Figure 1. The observed, calculated and difference profiles for the Rietveld refinement of  $\text{Nd}_{1.7}\text{Ba}_{0.3}\text{Ni}_{0.9}\text{Cr}_{0.1}\text{O}_{4+\delta}$  compound.

TABLE II. Structural parameters of  $\text{Nd}_{1.7}\text{Ba}_{0.3}\text{Cr}_{0.1}\text{Ni}_{0.9}\text{O}_{4+\delta}$  obtained from Rietveld refinements of powder XRD data.

Atoms	Wyckoff positions	x	y	z	$B_{\text{iso}} (\text{\AA}^2)$
Nd/Ba	4e	0	0	0.36006(4)	1.215(25)
Ni/Cr	2a	0	0	0	1.369(51)
O2	4c	0	1/2	0	1.837(2)
O1	4e	0	0	0.1770(6)	5.001(2)

The  $(\text{Ni/Cr})\text{O}_6$  octahedra shares corners in the  $ab$ -plane forming a two-dimensional array of  $(\text{Ni/Cr})\text{-O}(\text{Ni/Cr})$  bonds, which is responsible for a variety of interesting physical phenomena, such as, the anisotropic electrical transport and magnetic exchange interactions (Bassat *et al.*, 1987; Buttrey and Honig, 1988).

The neodymium and barium atoms are surrounded by nine oxygen atoms (Figure 2). By examining the nine  $(\text{Nd/Ba})\text{-O}$  bonds, it should be noted that all of them present distances lying between 2.2837 and 2.7440  $\text{\AA}$  slightly lower than the sum of the ionic radii of  $\text{Ba}^{2+}$  ( $R_{\text{Ba}^{2+}} = 1.47 \text{ \AA}$ ) and  $\text{O}^{2-}$  ( $R_{\text{O}^{2-}} = 1.42 \text{ \AA}$ ) given by Shannon (1976). This result confirms the prevalence of the covalent character of these bonds. The interatomic distances and bond angles for  $\text{Nd}_{1.7}\text{Ba}_{0.3}\text{Ni}_{0.9}\text{Cr}_{0.1}\text{O}_{4+\delta}$  compound are listed in Table III.

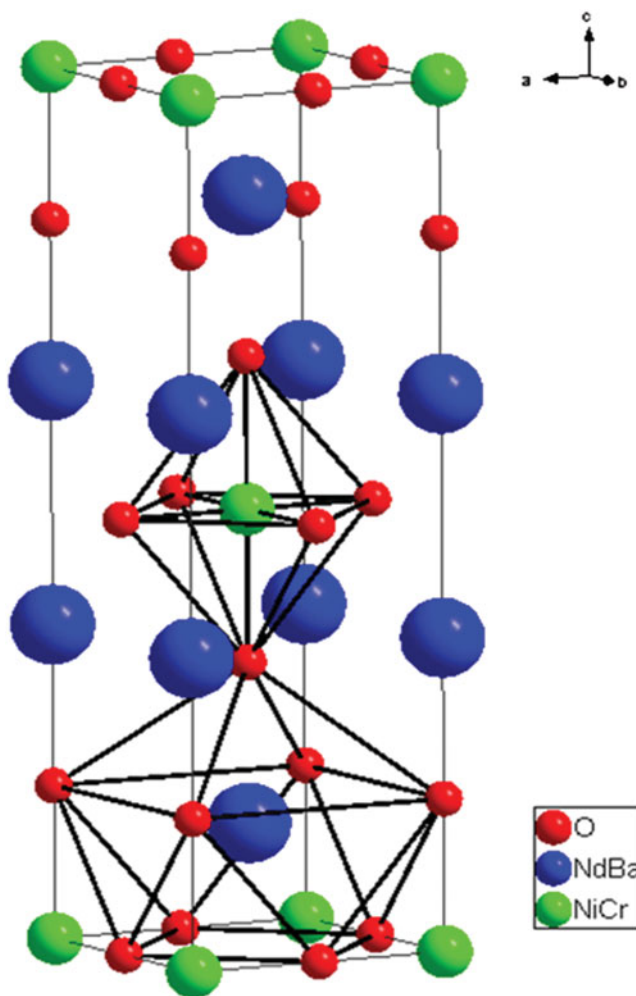


Figure 2. Crystal structure of  $\text{Nd}_{1.7}\text{Ba}_{0.3}\text{Ni}_{0.9}\text{Cr}_{0.1}\text{O}_{4+\delta}$  sample with the tetragonal  $\text{K}_2\text{NiF}_4$ -type structure.



TABLE III. The interatomic distances and bond angles for  $\text{Nd}_{1.7}\text{Ba}_{0.3}\text{Ni}_{0.9}\text{Cr}_{0.1}\text{O}_{4+\delta}$ .

Bond	Distance(Å)
Nd/Ba–O1	2.7440(1) × 4
Nd/Ba–O2	2.5895(4) × 4
Nd/Ba–O1	2.2837(8) × 1
Ni/Cr–O2	1.9125(0) × 4
Ni/Cr–O1	2.2081(8) × 2
	Angles(°)
O2–Cr/Ni–O2	90
O2–Cr/Ni–O2	90
O2–Cr/Ni–O2	180
O2–Cr/Ni–O1	90
O1–Cr/Ni–O1	180
O1–Nd/Ba–O2	132.39(1)
O2–Nd/Ba–O1	128.95(1)
O2–Nd/Ba–O1	66.36(1)
O1–Nd/Ba–O1	88.38(1)
O2–Nd/Ba–O2	62.976(0)
O2–Nd/Ba–O2	95.236(0)
O1–Nd/Ba–O1	80.29(1)
O1–Nd/Ba–O1	160.58(1)

The prominent feature of perovskite structures is their flexibility with respect to relative cation size. This is generally achieved by tilting of the  $BX_6$  octahedral centre, leading to slight distortions of the octahedra (Elcombe *et al.*, 1991). The (Ni/Cr)–O6 octahedra are untilted for the present structure model of  $\text{Nd}_{1.7}\text{Ba}_{0.3}\text{Ni}_{0.9}\text{Cr}_{0.1}\text{O}_{4+\delta}$ , compared with  $\text{Nd}_{1.7}\text{Ba}_{0.3}\text{NiO}_{4+\delta}$  (Takeda *et al.*, 1992). Thus, the distances (Ni/Cr)–O:  $d(\text{Ni/Cr})\text{-O}_{\text{apical}} = 2.2081 \text{ \AA}$  and  $d(\text{Ni/Cr})\text{-O}_{\text{planar}} = 1.9125 \text{ \AA}$  are very close to  $\text{Nd}_{1.7}\text{Ba}_{0.3}\text{NiO}_{4+\delta}$  [ $d(\text{Ni/Cr})\text{-O}_{\text{apical}} = 2.20 \text{ \AA}$  and  $d(\text{Ni/Cr})\text{-O}_{\text{planar}} = 1.91 \text{ \AA}$ ]. By substituting Ni with Cr, we assist in little changes in the unit-cell parameters that may mainly result from the small differences in ionic size of  $\text{Ni}^{3+}/\text{Ni}^{2+}$  and  $\text{Cr}^{3+}/\text{Cr}^{4+}$ .

### C. Electrical conductivity

To obtain dense ceramic pellets for electrical measurements, powder sample of the material was grounded (in ethanol). A pellet (13 mm in diameter and 1.8 mm thick) was prepared by uniaxial pressing (100 MPa). It was then sintered at 1373 K for 2 h to obtain a disc with high density. The total electrical conductivity  $\sigma$  of sintered ceramic was determined under air using the four-probe technique in the temperature range between 313 and 708 K.

The crystal structure of  $\text{Nd}_{1.7}\text{Ba}_{0.3}\text{Ni}_{0.9}\text{Cr}_{0.1}\text{O}_{4+\delta}$  is made up of alternating rock-salt  $(\text{Nd/Ba})_2\text{O}_2$  and perovskite Ni/CrO<sub>2</sub> layers, and can accommodate a significant oxygen excess. The extra  $\text{O}^{2-}$  anions occupy interstitial positions in the (Nd/Ba)O bilayers. The equilibrium oxygen hyperstoichiometry ( $\delta$ ) in air is close to 0.06 at 300 K. The excess negative charge introduced by excess oxygen is neutralized by oxidation of Ni/Cr ions. As a result, the introduction of excess oxygen in the (Nd/Ba)O bilayers creates mobile holes in Ni/CrO<sub>6</sub> octahedra. The increase in electrical conductivity with temperature can be explained by the increasing mobility of oxygen interstitials and holes.

The corresponding curve to  $\sigma$  vs.  $T$  is reported in Figure 3. The conductivity, increases with temperature in the whole range of temperature.

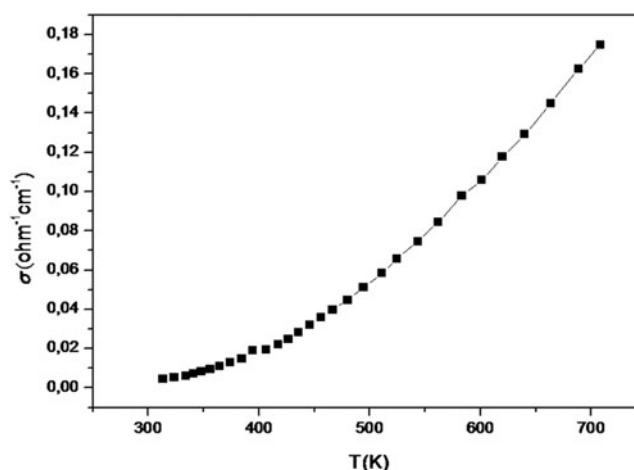


Figure 3. Thermal variation of the electric conductivity  $\sigma$  for the  $\text{Nd}_{1.7}\text{Ba}_{0.3}\text{Ni}_{0.9}\text{Cr}_{0.1}\text{O}_{4+\delta}$  compound ( $313 \text{ K} \leq T \leq 708 \text{ K}$ ).

Figure 4 shows the relationship of  $\ln(\sigma T)$  vs.  $1000/T$  for temperature range of 313–708 K. The increase in  $\ln(\sigma T)$  with increasing temperature indicates that the sample has semi-conductive behaviour at high temperature. To determine the conduction mechanism, we tried to use the thermally activated adiabatic small polaron hopping as the conduction model:

$$\sigma = \sigma_0 T^{-1} \exp\left(\frac{-E_a}{k_B T}\right)$$

where  $E_a$  is the activation energy (polaron formation and hopping energy),  $\sigma_0$  is a constant related to polaron concentration and diffusion. In the analysis of simulated curve:  $\ln(\sigma T) = f(1000/T)$ , we found that the convergence of the curve fitting was achieved in the whole range of temperature. This result implies that the transport properties in  $\text{Nd}_{1.7}\text{Ba}_{0.3}\text{Ni}_{0.9}\text{Cr}_{0.1}\text{O}_{4+\delta}$ , and in the temperature range of 313–708 K, are well described by the adiabatic small polaron hopping mechanism, where activation energy, after fitting, is  $E_a = 0.013 \text{ eV}$ .

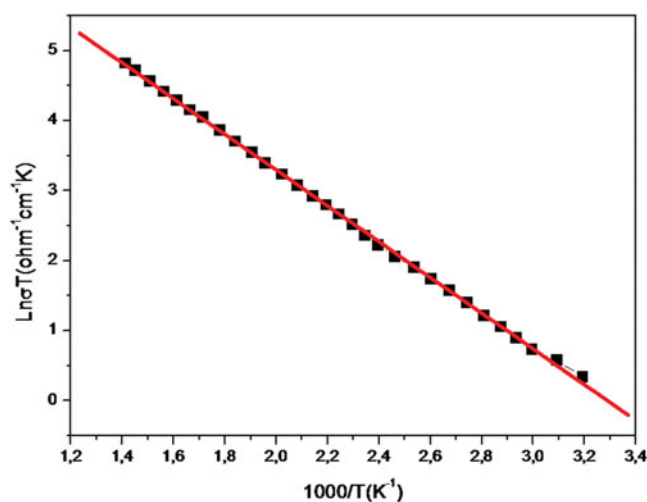


Figure 4. Arrhenius relations of  $\ln(\sigma T)$  vs.  $1000/T$  for the  $\text{Nd}_{1.7}\text{Ba}_{0.3}\text{Ni}_{0.9}\text{Cr}_{0.1}\text{O}_{4+\delta}$ . The solid lines are the fitting curves of equation, and the points represent the experimental values.

By comparing the transport properties at high temperature between  $\text{Nd}_{1.7}\text{Ba}_{0.3}\text{Ni}_{0.9}\text{Cr}_{0.1}\text{O}_{4+\delta}$  and  $\text{Nd}_{1.7}\text{Ba}_{0.3}\text{NiO}_{4+\delta}$  samples, one can conclude that both samples show a semi-conductive behaviour, and partial substitution of the Ni by Cr decreases significantly the conductivity. Taking into account that both compounds have the same amount of oxygen hyperstoichiometry ( $\delta$ ), we can conclude that the mobility of oxygen interstitials remains unchanged, consequently holes concentration is reduced. This behaviour, contrary to the  $\text{Nd}_{2-x}\text{Ba}_x\text{NiO}_{4+\delta}$  cases (Takeda *et al.*, 1992), may suggest an important role of hole trapping by the chrome cations forming stable  $\text{Cr}^{3+}$  states. Such hypothesis seems well supported by numerous experimental data on the oxygen non-stoichiometry and phase stability of various  $\text{LaSrCrO}_4$ -,  $\text{LaSrNiO}_4$ -,  $\text{LaSrCrO}_3$ - and  $\text{LaSrNiO}_3$ -based solid solutions, which suggest a considerably higher stability of  $\text{Cr}^{3+}$  compared to  $\text{Ni}^{3+}$  (Sauvet and Irvine, 2004; Millburn and Rosseinsky, 1997).

#### IV. CONCLUSION

$\text{Nd}_{1.7}\text{Ba}_{0.3}\text{Ni}_{0.9}\text{Cr}_{0.1}\text{O}_{4+\delta}$  compound was formed by sol-gel route and annealing at 1523 K in argon atmosphere. Rietveld refinement using powder XRD data shows that the title compound crystallizes in the tetragonal  $\text{K}_2\text{NiF}_4$ -type structure in space group  $I4/mmm$ . The results obtained by iodometric titration indicate excess oxygen in the sample. The investigation into the transport properties indicates that the electrical conductivity of  $\text{Nd}_{1.7}\text{Ba}_{0.3}\text{Ni}_{0.9}\text{Cr}_{0.1}\text{O}_{4+\delta}$  ceramic increased with increasing temperature. A semi-conductive behaviour is observed and the fitting shows that the adiabatic small polaron hopping model describes the experimental data in the temperature range between 313 and 708 K with an activation energy  $E_a = 0.013$  eV. By comparing the values of conductivities at high temperatures between  $\text{Nd}_{1.7}\text{Ba}_{0.3}\text{NiO}_{4+\delta}$  and  $\text{Nd}_{1.7}\text{Ba}_{0.3}\text{Ni}_{0.9}\text{Cr}_{0.1}\text{O}_{4+\delta}$  samples, it was concluded that the substitution of Ni by Cr significantly decreases the conductivity.

Arbuckle, B. W., Ramanujachary, K. V., Zhang, Z., and Greenblatt, M. (1990). "Investigation on the structural electrical and magnetic properties of  $\text{Nd}_{2-x}\text{Sr}_x\text{NiO}_{4+\delta}$ ," *J. Solid State Chem.* **88**, 278–290.

Bassat, J. M., Odier, P., and Gervais, F. (1987). "Two-dimensional plasmons in nonstoichiometric  $\text{La}_2\text{NiO}_4$ ," *Phys. Rev. B* **35**, 7126–7128.

Boultif, A. and Louër, D. (1991). "Indexing of powder diffraction patterns for low-symmetry lattices by the successive dichotomy method," *J. Appl. Crystallogr.* **24**, 987–993.

Buttrey, D. J. and Honig, J. M. (1988). "Influence of nonstoichiometry on the magnetic properties of  $\text{Pr}_2\text{NiO}_4$  and  $\text{Nd}_2\text{NiO}_4$ ," *J. Solid State Chem.* **72**, 38–41.

Buttrey, D. J., Honig, J. M., and Rao, C. N. R. (1986). "Magnetic properties of quasi-two-dimensional  $\text{La}_2\text{NiO}_4$ ," *J. Solid State Chem.* **64**, 287–295.

Chaker, H., Roisnel, T., Potel, M., and Ben Hassen, R. (2004). "Structural and electrical changes in  $\text{NdSrNiO}_{4-\delta}$  by substitute nickel with copper," *J. Solid State Chem.* **177**, 4067–4072.

Chaker, H., Roisnel, T., Cador, O., Amami, M., and Ben Hassen, R. (2006). "Neutron powder diffraction studies of  $\text{NdSrNi}_{1-x}\text{Cu}_x\text{O}_{4-\delta}$  ( $0 \leq x \leq 1$ ) and magnetic properties," *J. Solid State Sci.* **8**, 142–148.

Chaker, H., Roisnel, T., Ceretti, M., and Ben Hassen, R. (2007). "The synthesis, structural characterization and magnetic properties of compounds in the  $\text{Ln}_2\text{O}_3$ -SrO-NiO-CuO system for  $\text{Ln} = \text{La, Nd, Gd, Dy, Ho}$  and Er," *J. Alloys Compd.* **43**, 116–122.

Chen, C. H., Cheong, S.-W., and Cooper, A. S. (1993). "Charge modulations in  $\text{La}_{2-x}\text{Sr}_x\text{NiO}_{4+\delta}$  Ordering of polarons," *Phys. Rev. Lett.* **71**, 2461–2464.

Demourgues, A., Wattiaux, A., Grenier, J. C., Pouchard, M., Soubeyroux, J. L., Dance, J. M., and Hagenmuller, P. (1993). "Electrochemical preparation and structural characterization of  $\text{La}_2\text{NiO}_{4+\delta}$  phases ( $0 \leq \delta \leq 0.25$ )," *J. Solid State Chem.* **105**, 458–468.

Elcombe, M. M., Kisi, E. H., Hawkins, K. D., White, T. J., Goadman, P., and Matheson, S. (1991). "Structure determinations for  $\text{Ca}_3\text{Ti}_2\text{O}_7$ ,  $\text{Ca}_4\text{Ti}_3\text{O}_{10}$ ,  $\text{Ca}_{3.6}\text{Sr}_{0.4}\text{Ti}_3\text{O}_{10}$  and a refinement of  $\text{Sr}_3\text{Ti}_2\text{O}_7$ ," *Acta Crystallogr. Sect. B: Struct. Sci.* **47**, 305–314.

Ganguly, P., and Rao, C. N. R. (1984). "Crystal chemistry and magnetic properties of layered metal oxides possessing the  $\text{K}_2\text{NiF}_4$  or related structures," *J. Solid State Chem.* **53**, 193–216.

Gopalakrishnan, J., Colsmann, G., and Reuter, B. (1977). "Studies on the  $\text{La}_{2-x}\text{Sr}_x\text{NiO}_4$  ( $0 \leq x \leq 1$ ) system," *J. Solid State Chem.* **22**, 145–149.

Hamdi, S., Ouni, S., Chaker, H., Rohlicek, J., and Ben Hassen, R. (2011). "Synthesis, structural and electrical characterizations of  $\text{DySr}_5\text{Ni}_{2.4}\text{Cu}_{0.6}\text{O}_{12-\delta}$ ," *J. Solid State Chem.* **11**, 2897–2901.

Jammali, M., Chaker, H., Cherif, K., and Ben Hassen, R. (2010). "Investigation on the structural and electrical properties of  $\text{NdSrNi}_{1-x}\text{Cr}_x\text{O}_{4+\delta}$  ( $0.1 \leq x \leq 0.9$ ) system," *J. Solid State Chem.* **183**, 1194–1199.

Jorgensen, J. D., Dabrowski, B., Pei, S. Y., Richards, D. R., and Hinks, D. G. (1989). "Structure of the interstitial oxygen defect in  $\text{La}_2\text{NiO}_4 + \delta$ ," *Phys. Rev. B* **40**, 2187–2199.

Millburn, J. E., and Rosseinsky, M. J. (1997). " $\text{LaSrCr}_x\text{Ni}_{1-x}\text{O}_{4+\delta}$ : crystal chemistry, magnetism, and the stabilization of  $\text{Ni}^I$  in an oxide environment," *Chem. Mater.* **9**, 511–522.

Odier, P., Nigara, Y., and Coutures, J. (1985). "Phase relations in the La-Ni-O system: influence of temperature and stoichiometry on the structure of  $\text{La}_2\text{NiO}_4$ ," *J. Solid State Chem.* **65**, 32–40.

Rodríguez-Carvajal, J. (1990). "XVth Congress of the International union of Crystallography," Proceedings of the Satellite Meeting on Powder Diffraction, Toulouse, p. 127.

Rodríguez-Carvajal, J., Martínez, J. L., and Pannetier, J. (1988). "Anomalous structural phase transition in stoichiometric," *Phys. Rev. B* **38**, 7148–7151.

Sauvet, A.L. and Irvine, J.T.S. (2004). "Catalytic activity for steam methane reforming and physical characterisation of  $\text{La}_{1-x}\text{Sr}_x\text{Cr}_{1-y}\text{Ni}_y\text{O}_{3-\delta}$ ," *Solid State Ionics* **167**, 1–8.

Shannon, R. D. (1976). "Revised effective ionic radii and systematic studies of interatomic distances in halide and chalcogenides," *Acta Crystallogr.* **32**, 751–767.

Sreedhar, K. and Rao, C. N. R. (1990). "Electrical and magnetic properties of  $\text{La}_{2-x}\text{Sr}_x\text{NiO}_4$ : a tentative phase diagram," *Mater. Res. Bull.* **25**, 1235–1242.

Takeda, Y., Kanno, R., Sakano, M., Yamamoto, O., Takano, M., Bando, Y., Akinaga, H., Takita, K., and Goodenough, J. B. (1990). "Crystal chemistry and physical properties of  $\text{La}_{2-x}\text{Sr}_x\text{NiO}_4$  ( $0 \leq x \leq 1$ )," *Mater. Res. Bull.* **25**, 293–306.

Takeda, Y., Nishijima, M., Imanishi, N., Kanno, R., Yamamoto, O., and Takano, M. (1992). "Crystal Chemistry and transport Properties of  $\text{Nd}_{2-x}\text{A}_x\text{NiO}_4$  (A = Ca, Sr, or Ba, ( $0 \leq x \leq 1.4$ )," *J. Solid State Chem.* **96**, 72–83.

Tonus, F., Bahout, M., Battle, P. D., Hansen, T., Henry, P. F., and Roisnel, T. (2010). "*In situ* neutron diffraction study of the high-temperature redox chemistry of  $\text{Ln}_{3-x}\text{Sr}_{1+x}\text{NiCrO}_{8-\delta}$  ( $\text{Ln} = \text{La, Nd}$ ) under hydrogen," *J. Mater. Chem.* **20**, 4103–4115.